Wave Motion 128 (2024) 103326

Contents lists available at ScienceDirect

Wave Motion

journal homepage: www.elsevier.com/locate/wamot

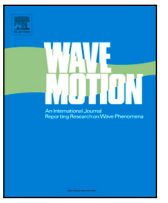

Highly localized horseshoe ripplons and solitons in positive dispersion media

Zhao Zhang [a], Qi Guo [a,*], Yury Stepanyants [b,*]

[a] Guangdong Provincial Key Laboratory of Nanophotonic Functional Materials and Devices, South China Normal University, Guangzhou 510631, PR China

[b] School of Mathematics, Physics and Computing, University of Southern Queensland, 487-535 West St., Toowoomba, QLD, 4350, Australia

ARTICLE INFO

Dedicated to the memory of Professor Noel Smyth

Keywords:
Kadomtsev–Petviashvili equation
Decaying solutions
Ripplons
Lumps

ABSTRACT

In this study, we systematically review various ripplon solutions to the Kadomtsev–Petviashvili equation with positive dispersion (KP1 equation). We show that there are mappings that allow one to transform the horseshoe solitons and curved lump chains of the KP1 equation into circular solitons of the cylindrical Korteweg–de Vries (cKdV) equation and two-dimensional solitons of the cylindrical Kadomtsev–Petviashvili (cKP) equation. Then, we present analytical solutions that describe new nonlinear highly localized ripplons of a horseshoe shape. Ripplons are two-dimensional waves with an oscillatory structure in space and a decaying character in time; they are similar to lumps but non-stationary. In the limiting case, the horseshoe ripplons reduce to solitons decaying with time and having bent fronts. Such entities can play an important role in the description of strong turbulence in plasma and other media.

"The ink of a scholar is more holy than the blood of a martyr." – Prophet Muhammad

1. Introduction

Currently, it is known the existence of numerous solutions to the KP equation — see, for example, Refs. [1–3] and references therein. Among them, one can mention solutions describing stationary formations such as plane solitons, lumps, and lump chains [4–9], as well as solutions describing resonant interactions between these formations [10–17]. There are also solutions to the KP equation dubbed ripplons [18–21]; they describe nonlinear excitations decaying in time and having an oscillatory structure in space. However, an interesting class of solutions – highly localized ripplons – has been missed. In this paper, we introduce such entities through exact and analytical solutions and investigate their properties.

The well-known KP equation can be presented in the traditional dimensionless form:

$$\left(u_t + 6uu_x + u_{xxx}\right)_x + 3\alpha^2 u_{yy} = 0. \tag{1.1}$$

Here subscripts x, y and t denote partial derivatives. The parameter α determines the type of the KP equation; when it is purely imaginary, $\alpha = i$, then Eq. (1.1) describes waves in positive dispersion media (e.g., waves in a magnetized plasma) and is dubbed KP1, whereas when it is purely real, $\alpha = 1$, then Eq. (1.1) describes waves in negative dispersion media (e.g., waves in oceans) and is dubbed KP2. Here we consider the former case with $\alpha^2 = -1$.

* Corresponding authors.
E-mail addresses: guoq@scnu.edu.cn (Q. Guo), Yury.Stepanyants@unisq.edu.au (Y. Stepanyants).

https://doi.org/10.1016/j.wavemoti.2024.103326
Received 6 February 2024; Received in revised form 19 March 2024; Accepted 28 March 2024
Available online 4 April 2024

Exact solutions to Eq. (1.1) can be constructed, for example, by means of the Zakharov–Shabat method [2,22] or through the Darboux–Matveev transform [3]. To this end, we use the formula derived in [4,18]:

$$u = 2\frac{\partial^2}{\partial x^2}\ln h(x,y,t), \tag{1.2}$$

where the auxiliary function $h(x,y,t)$ is presented through the determinant of an $M\times M$ matrix:

$$h(x,y,t) = \det\left[c_{jk} + \left\langle \phi_j^+, \phi_k^- \right\rangle\right] \tag{1.3}$$

with the matrix elements containing integrals:

$$\left\langle \phi_j^+, \phi_k^- \right\rangle = \int_x^{+\infty} \phi_j^+\left(x',y,t\right)\phi_j^-\left(x',y,t\right)dx', \tag{1.4}$$

and c_{jk} are arbitrary constants. Functions ϕ_j^+ are solutions to the linear set of equations:

$$\begin{aligned} &i\phi_y^+ + \phi_{xx}^+ = 0,\\ &\phi_t^+ + 4\phi_{xxx}^+ = 0, \end{aligned} \tag{1.5}$$

and functions ϕ_j^- are solutions to the complex conjugate set of equations.

Solutions to these linear equations can be presented in the exponential and polynomial-exponential forms:

$$\phi_j^+ = \left(\phi_j^-\right)^* = \sum_{s=1}^{N_1} A_{js}e^{\theta_{js}} + \sum_{s=1}^{N_2} B_{js}\frac{\partial}{\partial\lambda_{js}}e^{\theta_{js}} + \sum_{s=1}^{N_3} C_{js}\frac{\partial^2}{\partial^2\lambda_{js}}e^{\theta_{js}} + \cdots \tag{1.6}$$

Here asterisk stands for the complex conjugate and $\theta_{js} = \lambda_{js}x + i\lambda_{js}^2 y - 4\lambda_{js}^3 t$ and A_{js}, B_{js}, C_{js}, and λ_{js} are real constants.

The typical simplest solutions presented in such a form encompass line solitons [23], 2D solitons (lumps) [4,24], lump chains [6,7,25], and their stationary combinations [8,9,13,17,26]. Solutions based on functions (1.6) allow one to describe normal and resonance interactions of solitons, lumps, and lump chains [13,15–17,27]. There are also solutions that describe *ripplons*, i.e. solutions based on the Airy function $\mathrm{Ai}(z)$ that decay in time and have bent front with the oscillating structure in space (the details will be shown below). Such solutions were derived in different ways by Johnson & Tompson [18] and later by Nakamura [20]; we will call them *JTN ripplons*. JTN ripplons have a horseshoe shape but are not localized in space, their fronts last up to infinity.

In the hierarchy of these solutions, at least one class of localized ripplon-type solutions was missed. In this paper, we will fill in the gap and describe a variety of decaying solutions to the KP1 equation and present our recent advancements in this field. In Section 2, we outline JTN ripplons and horseshoe solitons with a subsequent discussion on their relation to the exact solutions of the cKdV equation. In Section 3, we revisit recently derived lump-chain ripplons [21] and transform them into two-dimensional solitons and circular lump chains of the cKP equation via an appropriate mapping. The lump-like ripplons are revisited in Section 4 with the notation that they correspond to exact solutions of the cKP1 equation. In Section 5, we introduce new ripplon solutions and horseshoe solitons that are localized in space. In the Conclusion, we discuss the results obtained in this paper.

2. JTN ripplons

As aforementioned, solutions in the form of Eq. (1.6) are not unique; there are other solutions to the linear set of Eqs. (1.5). Johnson & Thompson [18] and independently Nakamura [20] have found a solution to Eqs. (1.5) in the form:

$$\phi^+ = \rho\,(12t)^{-1/3}\mathrm{Ai}\,(Z)\,e^{i\theta}, \quad \phi^- = \rho\,(12t)^{-1/3}\mathrm{Ai}\,(Z)\,e^{-i\theta}, \tag{2.1}$$

where $\mathrm{Ai}(Z)$ is the Airy function of the first kind, ρ is an arbitrary real parameter, and

$$Z(x,y,t) = (12t)^{-1/3}\left(x - \frac{y^2}{12t}\right), \quad \theta(x,y,t) = \frac{y}{12t}\left(x - \frac{y^2}{18t}\right).$$

This solution represents a ripplon (the term was introduced by Nakamura [20]), a non-singular ripple that slowly decays with time as $t^{-2/3}$, whereas its characteristic scale increases as $t^{1/3}$ [18,20,21]. The auxiliary function of the simplest ripple-type solution is:

$$h = 1 + \rho^2(12t)^{-2/3}\int_x^{+\infty}\mathrm{Ai}^2\,(Z)\,\mathrm{d}x = 1 + \frac{\rho^2}{\sqrt[3]{12t}}\left\{\left[\mathrm{Ai}'\,(Z)\right]^2 - Z\mathrm{Ai}^2\,(Z)\right\}, \tag{2.2}$$

where Ai' is the derivative of the Airy function with respect to its argument. One can prove that function $h(x,y,t)$ in Eq. (2.2) is essentially positive for $t>0$; this secures the non-singularity of the ripplon solution shown in Fig. 1. The solution is not localized in space; at any fixed time moment, the ripplon amplitude is constant along the line $Z(x,y,t) = \text{constant}$. However, the line curvature decreases with time $x = y^2/(12t) + C$ where C is some constant. For a big $|Z|$, the ripplon solution has the following asymptotics:

$$u \sim \begin{cases} \dfrac{\sqrt[3]{12}}{6t^{2/3}\sqrt{|Z|}}\cos\left(\dfrac{4}{3}|Z|^{3/2}\right), & Z\to-\infty,\\[2ex] \dfrac{\rho^2}{12\pi t}\exp\left(-\dfrac{4Z^{3/2}}{3}\right), & Z\to+\infty. \end{cases} \tag{2.3}$$

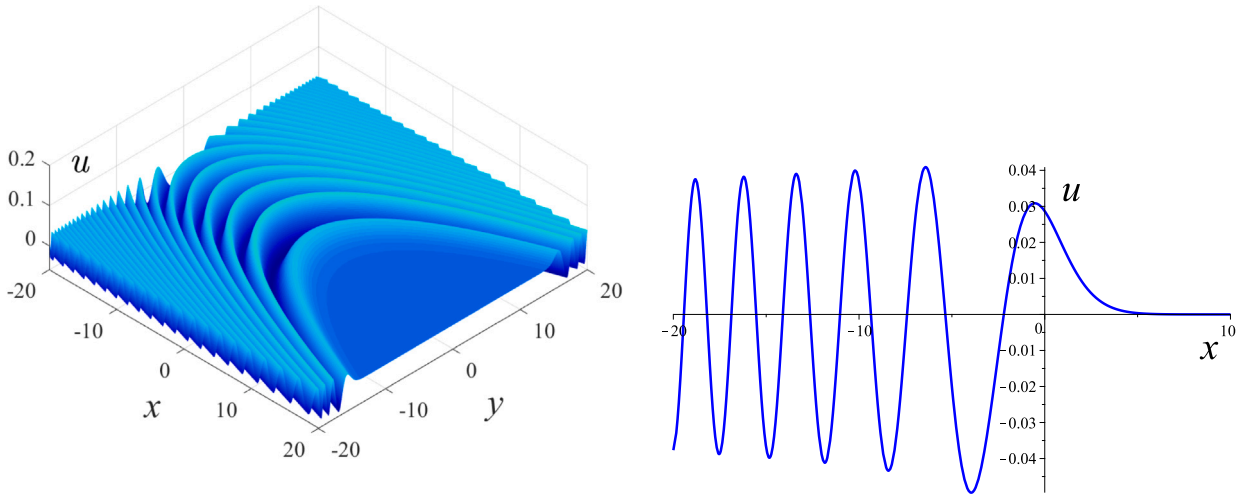

(a) Three-dimensional plot of a non-localised ripplon. (b) Cross-section of the ripplon at $y = 0$.

Fig. 1. Horseshoe ripplon solution (2.2) with $\rho = 1$ at $t = 1$.

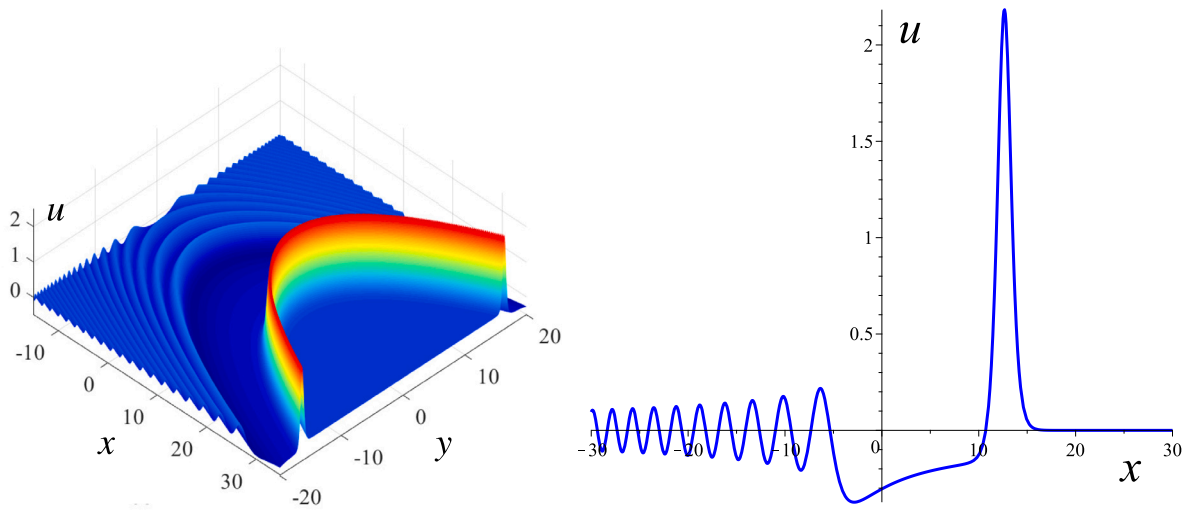

a) Three-dimensional plot of a horseshoe soliton. (b) Cross-section of the horseshoe soliton at $y = 0$.

Fig. 2. Horseshoe soliton as per Eq. (2.2) with $\rho = 10^5$ at $t = 1$.

As one can see from these formulae, the JTN ripplon decays rather slowly as $u \sim |Z|^{-1/2}$ when $Z \to -\infty$; therefore the integral in the infinite limits $\int u^2 dx$ does not converge, whereas the integral $\int u\, dx$ converges.

For a big value of the parameter ρ, the ripplon solution reduces to the solution describing a decaying soliton of a horseshoe shape in space [21] — see Fig. 2.

Note that the solution for the JTN ripplon can be derived from the exact solution of the cylindrical Korteweg–de Vries (cKdV) equation [28–32] through the simple change of variables. As was shown by Johnson [33] (see also [21,34,35]), all solutions to the cKdV equation,

$$v_r + 6vv_\tau + v_{\tau\tau\tau} + \frac{v}{2r} = 0, \tag{2.4}$$

can be transferred to the solutions of KP equation by means of the transformation:

$$\tau = x + \frac{y^2}{12\alpha^2 t}, \quad r = t. \tag{2.5}$$

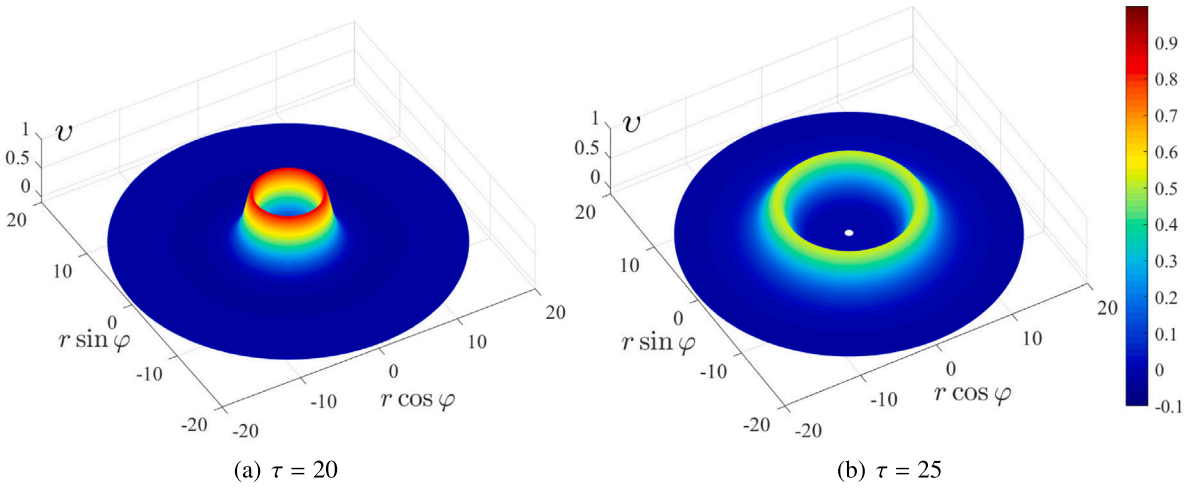

Fig. 3. Solution to the cKdV equation (2.6) in the form of a cylindrical outgoing soliton with the following parameters: $\rho = 10^5$ and $\tau_0 = 0$. Here r is the radial variable and φ — the polar angle.

Solution of the KP1 equation with the auxiliary function (2.2) can be transformed into the ring soliton of the cKdV equation (2.4) through the mapping (2.5):

$$\upsilon = 2\frac{\partial^2}{\partial\tau^2}\ln H(\tau, r), \quad H = 1 + \frac{\rho^2}{\sqrt[3]{12r}}\left\{\left[\mathrm{Ai}'(X)\right]^2 - X\mathrm{Ai}^2(X)\right\}, \tag{2.6}$$

where $X = (\tau - \tau_0)/\sqrt[3]{12r}$, and $\rho \gg 1$. The amplitude of this ring wave decays with a distance as $r^{-2/3}$, see Fig. 3. More details on exact solutions to the cKdV equations can be found in Refs. [28–32,36].

3. Ripplon chains

Because the system of Eqs. (1.5) is linear then, one can obtain another particular solution in the form of a linear combination of two functions like in Eq. (2.1) with different parameters. The corresponding auxiliary function $h(x, y, t)$ as per Eq. (1.3) is:

$$\begin{aligned} h(x,y,t) = {} & 2\rho_1\rho_2\frac{\mathrm{Ai}(Z_1)\,\mathrm{Ai}'(Z_2) - \mathrm{Ai}'(Z_1)\,\mathrm{Ai}(Z_2)}{x_1 - x_2}\cos\left[\frac{(y+y_0)(x_1-x_2)}{12t}\right] \\ & + \frac{\rho_1^2}{\sqrt[3]{12t}}\left\{\left[\mathrm{Ai}'(Z_1)\right]^2 - Z_1\mathrm{Ai}^2(Z_1)\right\} + \frac{\rho_2^2}{\sqrt[3]{12t}}\left\{\left[\mathrm{Ai}'(Z_2)\right]^2 - Z_2\mathrm{Ai}^2(Z_2)\right\}, \end{aligned} \tag{3.1}$$

where $Z_{1,2} = (x + x_{1,2})(12t)^{-1/3} - (y + y_0)^2(12t)^{-4/3}$, and $\rho_{1,2}$, $x_{1,2}$, and y_0 are arbitrary real parameters.

When $|\rho_2/\rho_1| \to 1$, Eq. (3.1) describes countless ripplon chains, consisting of lump chains that decay over time and bend in space as shown in Fig. 4(a). Chains curvatures gradually decrease with time. In another limit, when $|\rho_2/\rho_1| \to 0$, Eq. (3.1) describes a lump chain with constant amplitude lumps accompanied by a small amplitude decaying oscillatory tail (see Fig. 4(b)). The distance between lumps gradually increases with time; more details of this solution can be found in Ref. [21].

There is one more mapping (the LMS mapping after Lipovskii, Matveev, and Smirnov [37])

$$t = r, \quad x = \tau - \frac{r\varphi^2}{12\alpha^2}, \quad y = r\varphi \tag{3.2}$$

that allows one to transfer the KP equation (1.1) into the cylindrical Kadomtsev–Petviashvili (cKP) equation:

$$\frac{\partial}{\partial\tau}\left(\frac{\partial\upsilon}{\partial r} + 6\upsilon\frac{\partial\upsilon}{\partial\tau} + \frac{\partial^3\upsilon}{\partial\tau^3} + \frac{\upsilon}{2r}\right) + \frac{3\alpha^2}{r^2}\frac{\partial^2\upsilon}{\partial\varphi^2} = 0. \tag{3.3}$$

Using the mapping (3.2) with $\alpha = i$, a solution with the auxiliary function (3.1) can be transferred into a lump chain of the cKP equation:

$$\upsilon = 2\frac{\partial^2}{\partial\tau^2}\ln H(r, \tau, \varphi), \tag{3.4}$$

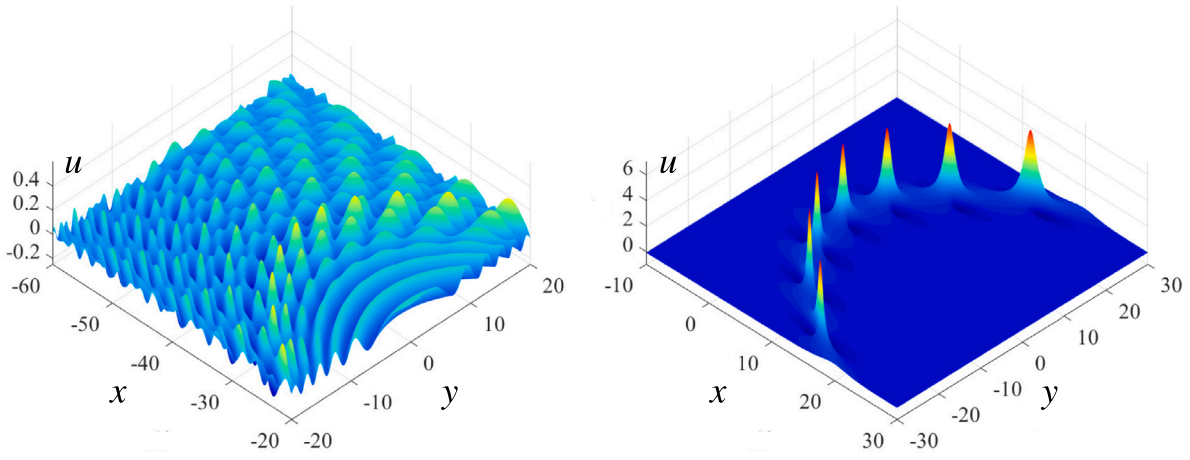

(a) Lump-chain ripple (b) Curved lump chain

Fig. 4. Surface plot of the solution to the KP1 equation with the auxiliary function (3.1). Panel (a) shows countless sets of lump chains with the choice of parameters $\{t = 2,\ x_1 = 36,\ x_2 = 0,\ \rho_1 = 1,\ \rho_2 = -1\}$; panel (b) shows one lump chain with constant amplitude lumps; the parameters are: $\{t = 4,\ x_1 = 36,\ x_2 = 0,\ \rho_1 = 1,\ \rho_2 = -10^{-10}\}$. The trailing oscillatory tail accompanying the lump chain is invisible in this figure due to the small amplitude and big distance from the chain.

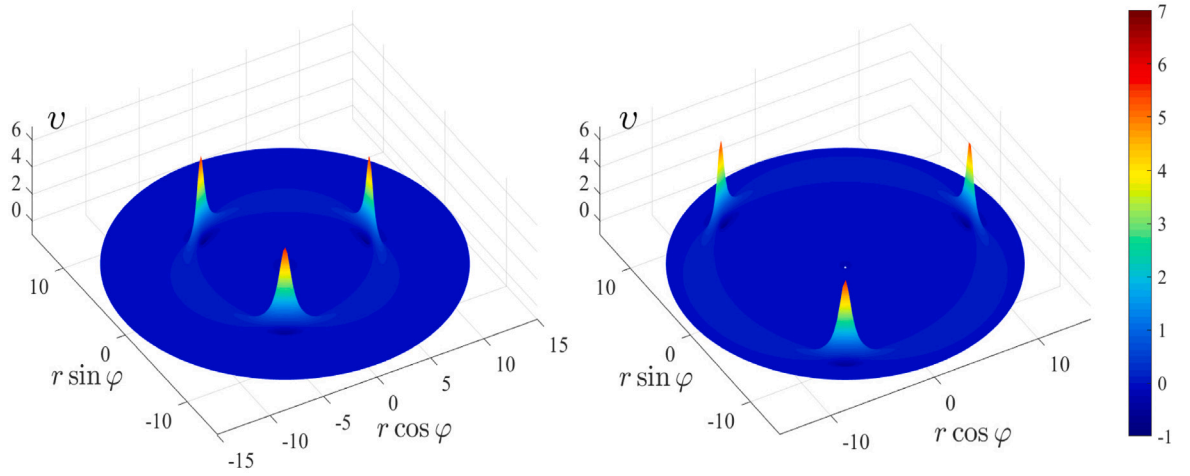

(a) $\tau = 20$ (b) $\tau = 40$

Fig. 5. Solution of the cKP equation (3.4) at two different time with the following parameters: $\tau_1 = 36,\ \tau_2 = 0,\ \rho_1 = 1,\ \rho_2 = -10^{-10}$.

with

$$H = 2\rho_1\rho_2 \frac{\mathrm{Ai}\left(X_1\right)\mathrm{Ai}'\left(X_2\right) - \mathrm{Ai}'\left(X_1\right)\mathrm{Ai}\left(X_2\right)}{\tau_1 - \tau_2} \cos\left(\frac{\tau_1 - \tau_2}{12}\varphi\right) + \frac{\rho_1^2}{\sqrt[3]{12r}}\left\{\left[\mathrm{Ai}'\left(X_1\right)\right]^2 - X_1\mathrm{Ai}^2\left(X_1\right)\right\} + \frac{\rho_2^2}{\sqrt[3]{12r}}\left\{\left[\mathrm{Ai}'\left(X_2\right)\right]^2 - X_2\mathrm{Ai}^2\left(X_2\right)\right\}.$$

This solution describes a lump chain consisting of $\left|\tau_1 - \tau_2\right|/12$ lumps (see Fig. 5) when $|\rho_2/\rho_1| \ll 1$. Here $X_{1,2} = \left(\tau + \tau_{1,2}\right)/\sqrt[3]{12r}$, and $\tau_{1,2}$ are real parameters. For the periodicity of the solution on the angular variable φ, $\left|\tau_1 - \tau_2\right|$ must be an integer multiple of 12.

With the help of the mapping (3.2) with $\alpha = i$, one can transform a horseshoe ripplon solution of the KP1 equation shown in Fig. 4 into multiple circular lump-chains of the cKP1 equation (3.3). The mapping can be used in the reverse order too to transform exact solutions of the cKP1 equation (see, for example, [36]) into the corresponding horseshoe lump or ripplon solutions of the KP1 equation.

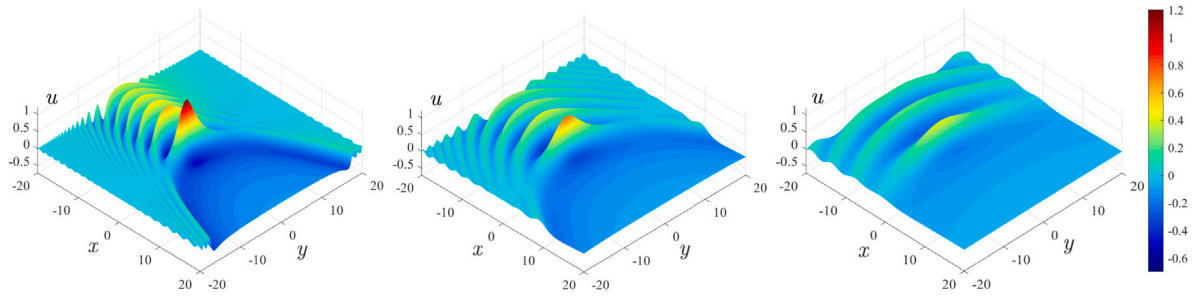

(a) $t = 1$ (b) $t = 2$ (c) $t = 5$

Fig. 6. Lump ripplons at different times as per solution with function (4.1), where $x_0 = y_0 = 0$.

4. Lump ripplons

An interesting solution describing ripplons with pronounced lumps riding on ripplons was recently obtained in Ref. [21]. This solution can be presented through the following auxiliary function:

$$h(x,y,t) = \frac{\rho^2}{36t}\left\{[Z\mathrm{Ai}(Z)]^2 - Z\left[\mathrm{Ai}'(Z)\right]^2 - 2\mathrm{Ai}(Z)\mathrm{Ai}'(Z) + 3\left(y+y_0\right)^2\frac{\left[\mathrm{Ai}'(Z)\right]^2 - Z\mathrm{Ai}^2(Z)}{(12t)^{\frac{4}{3}}}\right\}, \tag{4.1}$$

where $Z = (12t)^{-1/3}\left[x + x_0 - \left(y+y_0\right)^2/12t\right]$. Unlike the JTN ripplons discussed in Section 2, a solution with the auxiliary function (4.1) contains lumps sitting on each wavefront as illustrated by Fig. 6. Lump amplitudes gradually decrease in space as $u \sim |Z|^{-1/2}$ when $x \to -\infty$. The whole solution decays in time as $\sim t^{-2/3}$. We call such formations lump ripplons.

The solution describing the lump ripplon with the auxiliary function (4.1) can be formally transferred to the solution of the cKP equation through the mapping (3.2). However, the corresponding auxiliary function

$$H(r,\tau,\varphi) = \frac{\rho^2}{36r}\left\{[X\mathrm{Ai}(X)]^2 - X\left[\mathrm{Ai}'(X)\right]^2 - 2\mathrm{Ai}(X)\mathrm{Ai}'(X) + 3\varphi^2\frac{\left[\mathrm{Ai}'(X)\right]^2 - X\mathrm{Ai}^2(X)}{(12r)^{4/3}}\right\}, \tag{4.2}$$

where $X = \left(\tau+\tau_0\right)/\sqrt[3]{12r}$, is not periodic on the angular variable φ. Because of this, this solution, apparently, is out of physical meaning.

5. Highly localized ripplon solution

In this section, we derive new solutions to the KP1 equation that generalize the solution derived in Refs. [18,20] and contain both highly localized ripplons and horseshoe solitons. These solutions cannot be presented in terms of meaningful solutions to the cKdV equation or cKP equations by means of the Johnson transformation (2.5) or LMS transformation (3.2).

To this end, we note that the linear set of Eqs. (1.5) has a solution in the form (for details see Appendix):

$$\phi^+ = \rho\, t^{-1/3}\mathrm{Ai}\left(\zeta\right)e^{\Theta}, \quad \phi^- = \rho\, t^{-1/3}\mathrm{Ai}\left(\zeta^*\right)e^{\Theta^*}, \tag{5.1}$$

where $\zeta = \dfrac{a^2+4iay-4y^2}{48\sqrt[3]{12}t^{4/3}} + \dfrac{x}{\sqrt[3]{12}t}, \quad \Theta = \dfrac{(a+2iy)^3}{1728t^2} + \dfrac{x(a+2iy)}{24t}.$

Here $a > 0$ is a real parameter. The auxiliary function corresponding to the ripplon solution is:

$$h(x,y,t) = 1 + \frac{\rho^2}{t^{2/3}}\int_x^{+\infty}\mathrm{Ai}\left(\zeta\right)\mathrm{Ai}\left(\zeta^*\right)\exp\left[\frac{a}{2t}\left(x - \frac{12y^2-a^2}{432t}\right)\right]\mathrm{d}x. \tag{5.2}$$

The parameter a in Eq. (5.2) controls the degree of spatial localization of the ripplon; this is illustrated by Fig. 7. This figure shows that the tail in the cross-section $u(x,0,t)$ of the ripplon becomes shorter when the parameter a increases. If the parameter a is big enough then, there are no oscillatory tails behind the ripplon — see, for example, the cross-section of the ripplon with $a = 10$ in Fig. 7b). When $a \to 0$, the derived solution reduces to the nonlocalized JTN ripplon — see Fig. Fig. 7a). As one can see from Fig. 7(c), this solution is localized in all directions. It has a maximum at $y = 0$ and decreases along the front on both sides from the maximum owing to the exponential factor in Eq. (5.2).

The influence of the exponential factor diminishes when the time elapses. To a certain extent, this is equivalent to a decrease of the parameter a. As a result of this, the ripplon becomes wider with time, its oscillatory tail becomes longer, and the amplitude decreases. The leading maximum of the ripplon shifts to the left so that one can say that the ripplon gradually moves to the left and experiences dispersion spreading; this is demonstrated by Fig. 8.

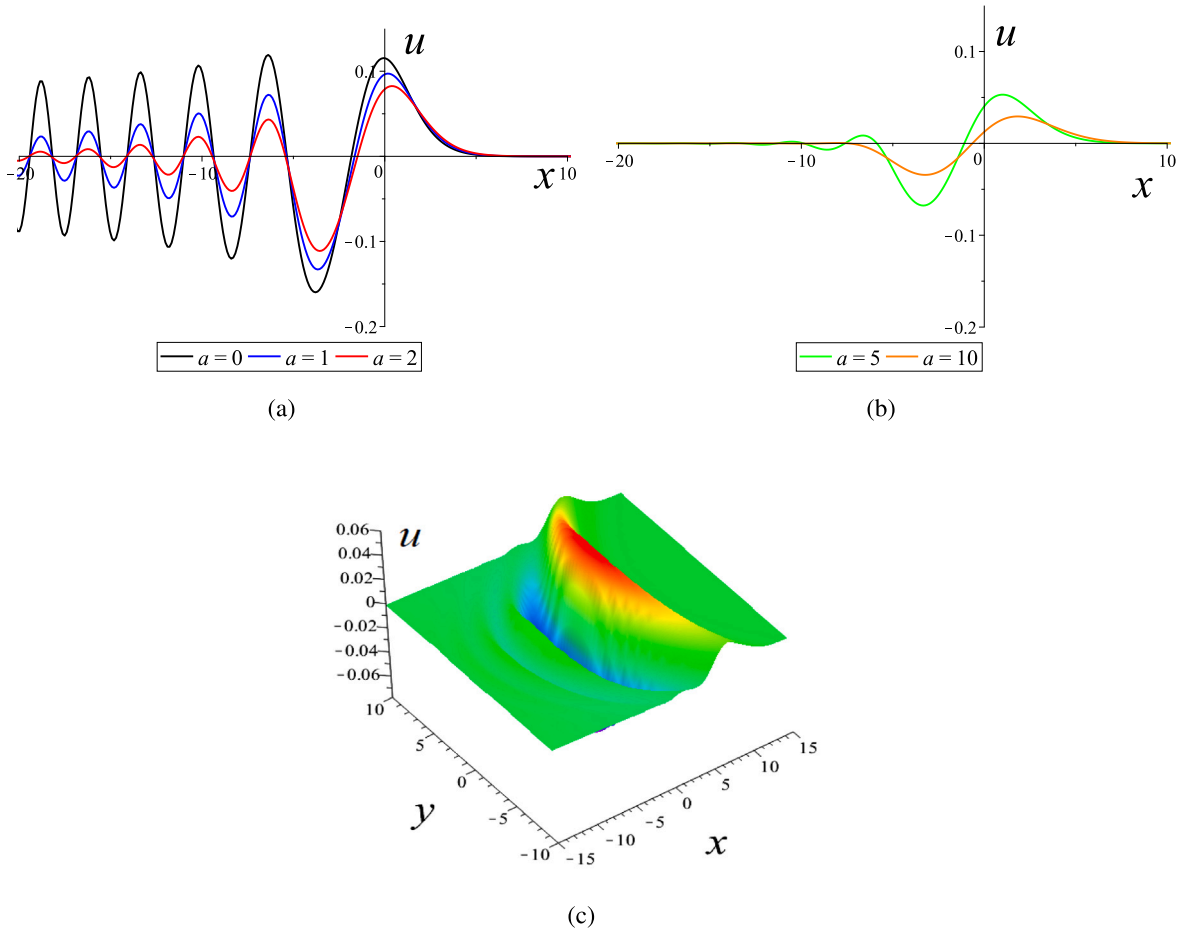

Fig. 7. Panels (a) and (b) show the cross-sections of the ripplon solution with the auxiliary function Eq. (5.2) at $y = 0$ (see the legends). Panel (c) shows the surface plot of the typical highly localized ripplon with $a = 4$. In all these panels, solutions were generated for $\rho = 1$ and $t = 1$.

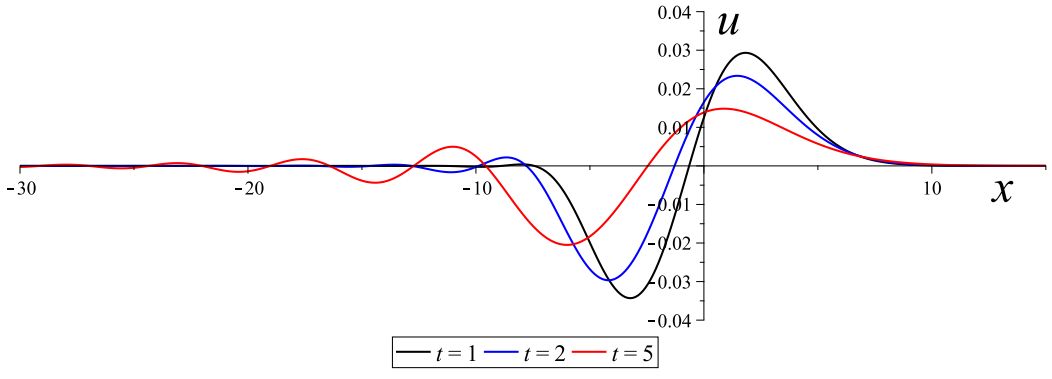

Fig. 8. The cross-section of the ripplon solution with the auxiliary function Eq. (5.2) for $y = 0$ at different time moments (see the legend). The plot was generated for $\rho = 1$ and $a = 10$.

Solution based on the auxiliary function (5.2) contains two free parameters. We have described the influence of the parameter a when $\rho = 1$, and now, we will demonstrate the effect of the parameter ρ when $a =$ constant. When ρ increases, the leading part in the ripplon cross-section becomes similar to the cross-section of the cylindrical soliton of the cKdV equation [32] — see Fig. 9. There is a long negative-polarity tail behind the leading pulse which ends up by small-amplitude ripples. Our estimates show that in

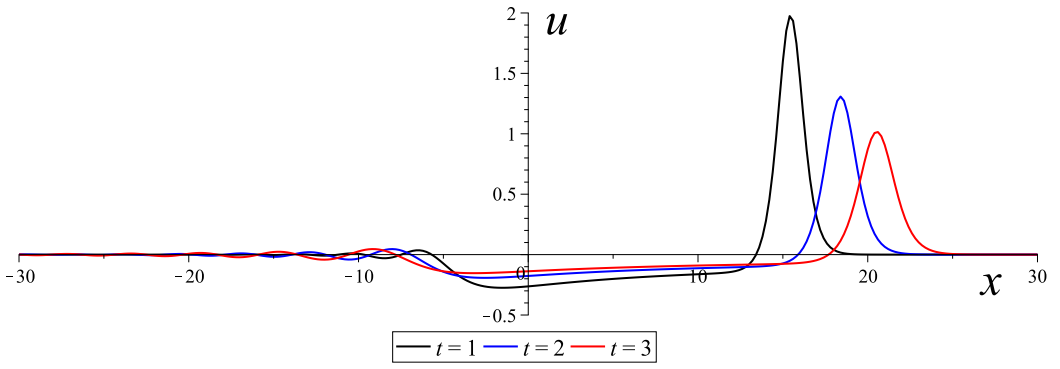

(a) A cross-section of a localised horseshoe soliton

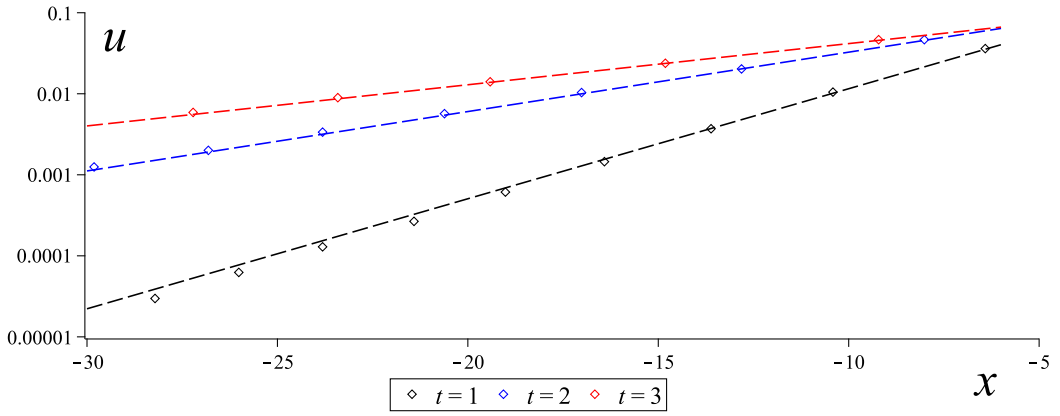

(b) Spatial decay of the ripplon tail shown in panel (a) at different time moments.

Fig. 9. (a) The cross-section of the ripplon solution with the auxiliary function Eq. (5.2) at $y = 0$ and different time moments (see the legend). The plot was generated for $\rho = 10^5$ and $a = 4$. (b) Sample points of local maxima in the oscillating tail behind the ripplons shown in panel (b). The best-fit approximation of the corresponding lines are $u = \exp(0.3127x - 1.3349)$ for $t = 1$, $u = \exp(0.1688x - 1.7354)$ for $t = 2$, and $u = \exp(0.1170x - 2.0094)$ for $t = 3$.

contrast to JTN and lump ripplons mentioned in Sections 2 and 4, ripples behind this highly localized ripplon decay exponentially with x but the decay rate depends on time, i.e. $u \sim \exp[g(t)x]$, where $g(t) > 0$ for $x \to -\infty$; see panel (b) in Fig. 9.

Fig. 10 illustrates a spatial structure of the solution that can be considered as the gradually decaying soliton with a horseshoe front (unfortunately, we were unable to present a smooth surface plot similar to that shown in Fig. 2 due to the computer memory restriction). The solution is highly localized and has a relatively high front curvature at small times (see Fig. 10a) but then when time elapses, the amplitude of the soliton and its curvature decrease; and it becomes wider in space (see Fig. 10b). The pulse moves to the right; the position of its maximum increases as $x_m \sim t^{1/3}$, whereas its amplitude decreases as $A_m \sim t^{-2/3}$. There is some deviation from these dependences at the early stage of evolution but after a short adjustment time, the asymptotic regime onsets. This is illustrated by Fig. 11.

It is worth noting that in contrast to the JTN and lump ripplons, the constructed solutions both for the highly localized ripplon and horseshoe soliton provide convergence of both integrals $\int u\,dx$ and $\int u^2 dx$ in infinite limits and, as a result, the convergence of two-dimensional integrals that are related to the mass and energy conservation:

$$I_1 = \iint_{-\infty}^{+\infty} u(x,y,t)\,dx\,dy, \quad I_2 = \iint_{-\infty}^{+\infty} u^2(x,y,t)\,dx\,dy. \tag{5.3}$$

These conserved quantities play an important role in physical applications.

In a similar way, one can construct ripplon-type solutions for the KP2 equation (Eq. (1.1) with $\alpha = 1$) but such solutions are singular for all parameters except $a = 0$. In the latter case, solutions were obtained in Refs. [18–21] and represent horseshoe solitons with a constant amplitude along the bent front. Qualitatively they look like a horseshoe ripplon shown in Fig. 1(a) or like a horseshoe soliton shown in Fig. 2(a) but with the fronts bent in the opposite direction. We do not consider here singular solutions because they are, apparently, out of physical interest.

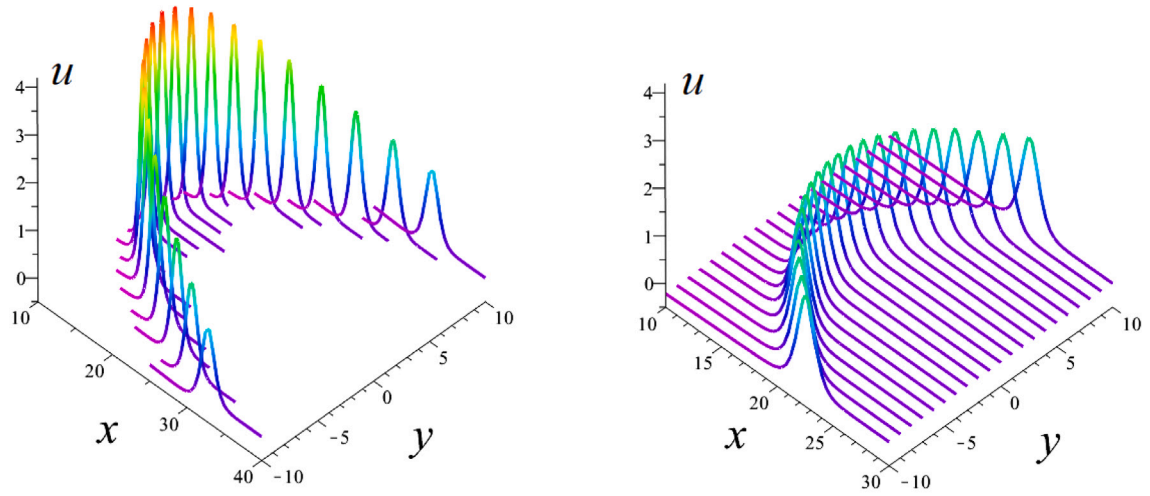

(a) $t = 1/4$ (b) $t = 1$

Fig. 10. The structure of the localized horseshoe soliton at two instants of time. The plot was generated on the basis of auxiliary function (5.1) with the following parameters: $\rho = 10^5$, $a = 4$.

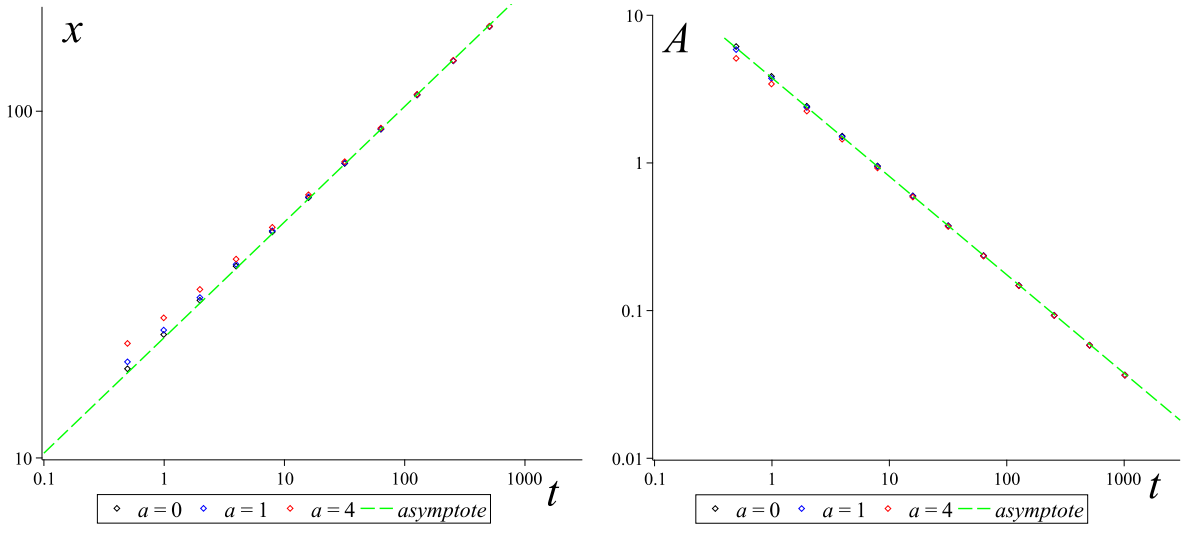

(a) The time dependence of the position of solution maximum $x_m(t)$.

(b) The time dependence of the maximum $A(t)$.

Fig. 11. Dependences of the maximum position (a) and amplitude (b) on time in log–log scale as per solution based on the auxiliary function (5.2) with $\rho = 10^{10}$ and different values of a — see the legends. The green lines are the asymptotes $\log x = 1.347 + \log t/3$ and $\log A = 0.576 - 2\log t/3$.

6. Conclusion

In this paper, we have systematically reviewed various ripplon-type solutions to the Kadomtsev–Petviashvili equation, including JTN ripplons (2.2), ripplon chains (3.1), and lump ripplons (4.1). At certain parameters, ripplon solutions can be reduced to horseshoe solitons and curved lump chains. These solutions can be mapped into circular solitons (2.6) of the cKdV equation using the Johnson transformation [33] or to two-dimensional solitons (3.4) of the cKP equation through the LMS transformation [37].

We have also constructed new analytic solutions that are completely localized in space. Within this class of solutions, wave shapes can vary from two-dimensional ripplons of a horseshoe shape to solitons with a bent front accompanied by long monotonic tails in the near-field (close to soliton maximum) and small-amplitude ripples in the far-field. All these entities gradually decay in time as $t^{-2/3}$. They are highly localized in space so that the "mass" and "energy" integrals (5.3) converge. Solutions contain a free

parameter that controls the degree of their localization; they become non-localized JTN ripplons [18–20] or decaying horseshoe solitons when this parameter vanishes.

Solutions derived can be of interest as elementary nonlinear modes existing in parallel with solitons and lumps in real physical media (plasma, solids, Bose–Einstein condensate, and others). An ensemble of such horseshoe highly localized ripplons and solitons can play an important role in the theory of strong turbulence. We plan to investigate further interactions of these kinds of ripplons/solitons with plane solitons and lumps.

CRediT authorship contribution statement

Zhao Zhang: Writing – review & editing, Writing – original draft, Visualization, Validation, Methodology, Investigation, Formal analysis, Conceptualization. **Qi Guo:** Writing – review & editing, Visualization, Validation, Supervision, Project administration, Conceptualization. **Yury Stepanyants:** Writing – review & editing, Writing – original draft, Validation, Methodology, Investigation, Formal analysis, Conceptualization.

Declaration of competing interest

The authors declare that they have no known competing financial interests or personal relationships that could have appeared to influence the work reported in this paper.

Data availability

No data was used for the research described in the article.

Acknowledgments

Qi Guo and Zhao Zhang acknowledge the financial support provided by the Natural Science Foundation of Guangdong Province of China (grant No. 2021A1515012214) and the Science and Technology Program of Guangzhou (grant No. 2019050001).

Appendix

In this Appendix, we describe how to derive solutions to Eqs. (1.5) for horseshoe ripplons, solitons, and some other solutions. Let us start with the first equation of the set (1.5):

$$i\phi_y^+ + \phi_{xx}^+ = 0. \tag{A.1}$$

In this equation, the time variable plays a role of a parameter. Using the solution for the non-localized horseshoe ripplons derived in [18–20] as the hint (see also [38]), we look for a solution to Eq. (A.1) in the form:

$$\phi^+ = \rho \mathrm{Ai}\,(q)\, e^w, \tag{A.2}$$

where $\mathrm{Ai}(q)$ is the Airy function ρ is a complex constant and q and w are functions of x, y, and t. Substituting function ϕ^+ into Eq. (A.1), we obtain an equation which contains the Airy function and its derivative only, $\mathrm{Ai}\,(q)$, $\mathrm{Ai}'\,(q)$. The second derivative of the Airy function can be expressed through the Airy function owing to its property, $\mathrm{Ai}''\,(q) = q\mathrm{Ai}\,(q)$. Then, we equate to zero the coefficients in front of $\mathrm{Ai}\,(q)$ and $\mathrm{Ai}'\,(q)$; this leads to the set of equations for q and w:

$$\begin{aligned} &q\left(\frac{\partial q}{\partial x}\right)^2 + i\frac{\partial w}{\partial y} + \left(\frac{\partial w}{\partial x}\right)^2 + \frac{\partial^2 w}{\partial x^2} = 0, \\ &i\frac{\partial q}{\partial y} + 2\left(\frac{\partial q}{\partial x}\right)\frac{\partial w}{\partial x} + \frac{\partial^2 q}{\partial x^2} = 0. \end{aligned} \tag{A.3}$$

Let us look for a solution to this set of equations in the form of polynomials:

$$q = \sum_{j,s=0}^{j+s=m} A_{js}(t) x^j y^s, \quad w = \sum_{j,s=0}^{j+s=m} B_{js}(t) x^j y^s, \tag{A.4}$$

where $A_{js}(t)$ and $B_{js}(t)$ are unknown complex coefficients that ought to be determined. They can be determined by substituting expressions (A.4) into Eq. (A.3) and equating to zero coefficients of each power of x and y.

With the help of symbolic computer manipulation, we get the solution to Eqs. (A.3) in the form:

$$\begin{aligned} &q(x,y) = \mathrm{Rt}\left(Z^3 + f_4\right)\left(f_4 y^2 - ix - \frac{if_3}{f_4}y - \frac{if_2}{f_4} + \frac{f_3^2}{4f_4^3}\right), \\ &w(x,y) = \frac{2i}{3}f_4^2 y^3 + f_4 xy + f_3 y^2 + f_2 y - \frac{if_3}{2f_4}x + f_1, \end{aligned} \tag{A.5}$$

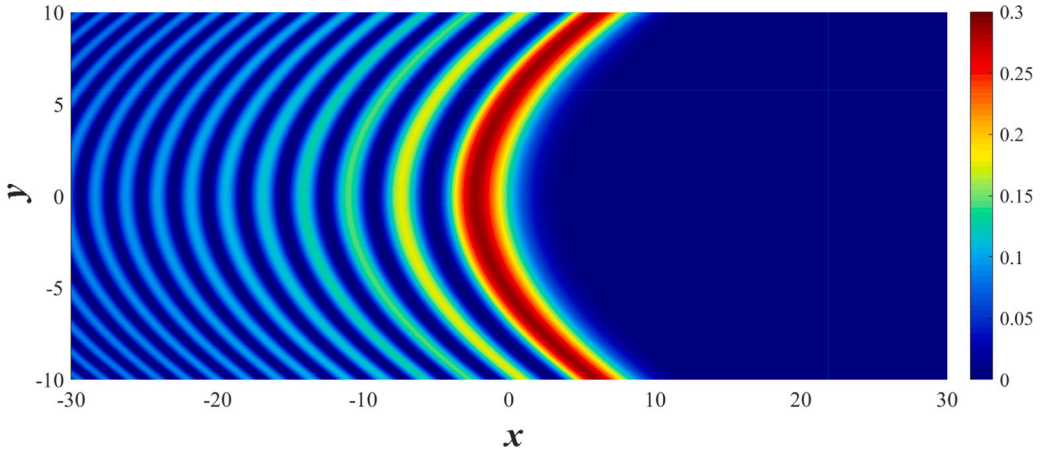

Fig. S1. Visualization of the squared modulus of the function (A.9), $|\phi^+|^2$, at $t = 1$. On the line $y = 0$, this function decays algebraically $\sim |x|^{-1}$ when $x \to -\infty$ and exponentially when $x \to +\infty$. Function values remain constant on each wavefront.

where $\mathrm{Rt}\left(Z^3 + f_4\right)$ is any one of the three complex roots of the equation $Z^3 + f_4 = 0$, and f_1, f_2, f_3, and f_4 are complex functions of t.

To determine functions f_i $(i = 1, 2, 3, 4)$, we substitute the expression for ϕ^+ from Eq. (A.2) into the second equation of the system (1.5). Then, we collect the coefficients in front of $\mathrm{Ai}\,(q)$ and $\mathrm{Ai}'\,(q)$ and equate them to zero. This gives a set of polynomial equations concerning x and y:

$$\begin{aligned} &\sum F_{1,ij}\left(f_1, f_2, f_3, f_4\right) x^i y^j = 0, \\ &\sum F_{2,ij}\left(f_1, f_2, f_3, f_4\right) x^i y^j = 0. \end{aligned} \tag{A.6}$$

By setting the coefficients of each power of x and y equal to zero, we obtain:

$$\begin{aligned} f_1(t) &= -\frac{ia_1a_2}{2t} - \frac{\ln t}{3} + \frac{a_1^3}{1728t^2} + a_3, \\ f_2(t) &= \frac{ia_1^2}{288t^2} + \frac{a_2}{t}, \\ f_3(t) &= -\frac{a_1}{144t^2}, \quad f_4(t) = \frac{i}{12t}. \end{aligned} \tag{A.7}$$

Therefore, the general form of the solution to Eqs. (1.5) is:

$$\begin{aligned} \phi^+ = {} & \frac{\rho}{\sqrt[3]{t}}\mathrm{Ai}\left[-i\,\mathrm{Rt}\left(Z^3 + \frac{i}{12t}\right)\left(x - 12ia_2 + \frac{a_1^2 + 4y(ia_1 - y)}{48}\right)\right] \\ & \times \exp\left[\frac{x\left(a_1 + 2iy\right) + 12a_2\left(2y - ia_1\right)}{24t} + \frac{a_1^3/6 + ia_1^2y - 2a_1y^2 - 4iy^3/3}{288t^2}\right], \end{aligned} \tag{A.8}$$

where a_1 and a_2 are arbitrary complex constants. The constant a_3 is unimportant, it can be absorbed in the constant ρ.

Owing to the homogeneity of Eqs. (1.5) and its autonomy (the coefficients are constant), the choice of the origin in each variable can be taken arbitrarily; this implies that function a ϕ^+ with the arbitrarily shifted coordinates, $x \to x + x_j$, $y \to y + y_j$, $t \to t + t_j$, remains a solution of Eqs. (1.5). It is clear also that the complex-conjugate function ϕ^- satisfies the complex-conjugate set of equations.

By choosing now some particular values of constants a_1, a_2, we can obtain different particular solutions. Below we present three typical cases that demonstrate different families of solutions.

(1) If we set $\mathrm{Rt}\left(Z^3 + i/12t\right) = i/\sqrt[3]{12t}$ and $a_1 = a_2 = 0$, we obtain function

$$\phi^+ = \frac{\rho}{\sqrt[3]{t}}\mathrm{Ai}\left[\frac{12xt - y^2}{(12t)^{4/3}}\right]\exp\left[\frac{iy\left(18\,xt - y^2\right)}{216t^2}\right]. \tag{A.9}$$

This function and its complex-conjugate provide the ripplon solution derived by Johnson & Thompson [18] and Nakamura [20] through the auxiliary function (2.2) (cf. Eq. (2.1) for ϕ^+). The spatial structure of the function $|\varphi^+|^2$ is shown in Fig. S1 for $\rho = 1$ and $t = 1$.

(2) If we set $\mathrm{Rt}\left(Z^3 + i/12t\right) = i/\sqrt[3]{12t}$, $a_1 \neq 0$, $a_2 = 0$, we obtain function

$$\phi^+ = \frac{\rho}{\sqrt[3]{t}}\mathrm{Ai}\left[\frac{a_1^2 + 4ia_1y - 4y^2}{48\sqrt[3]{12}t^{4/3}} + \frac{x}{\sqrt[3]{12t}}\right]\exp\left[\frac{\left(a_1 + 2iy\right)^3}{1728t^2} + \frac{\left(a_1 + 2iy\right)x}{24t}\right]. \tag{A.10}$$

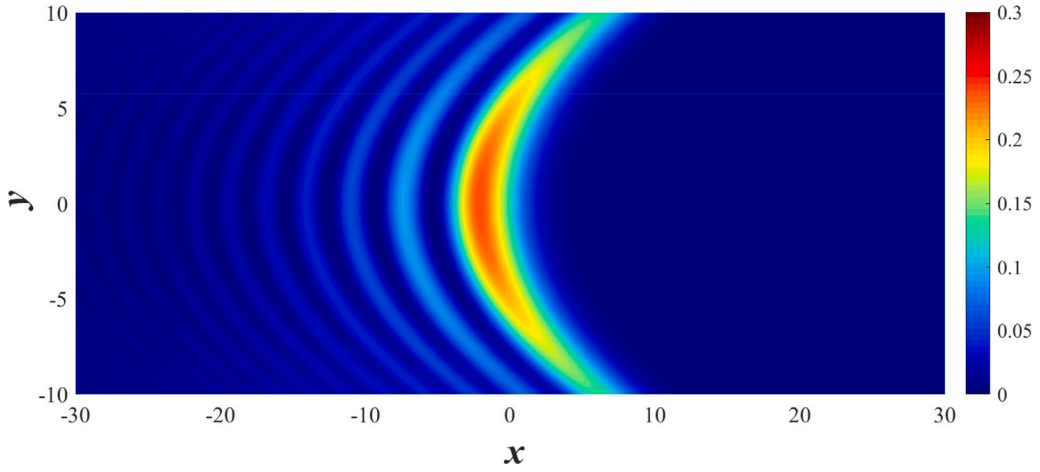

Fig. S2. Visualization of the squared modulus of the function (A.10) $|\phi^+|^2$ with $a_1 = 1$ at $t = 1$. This function $|\phi^+|^2$ decays exponentially at $|x| \to \infty$, and its values vary along the fronts havin maxima at $y = 0$.

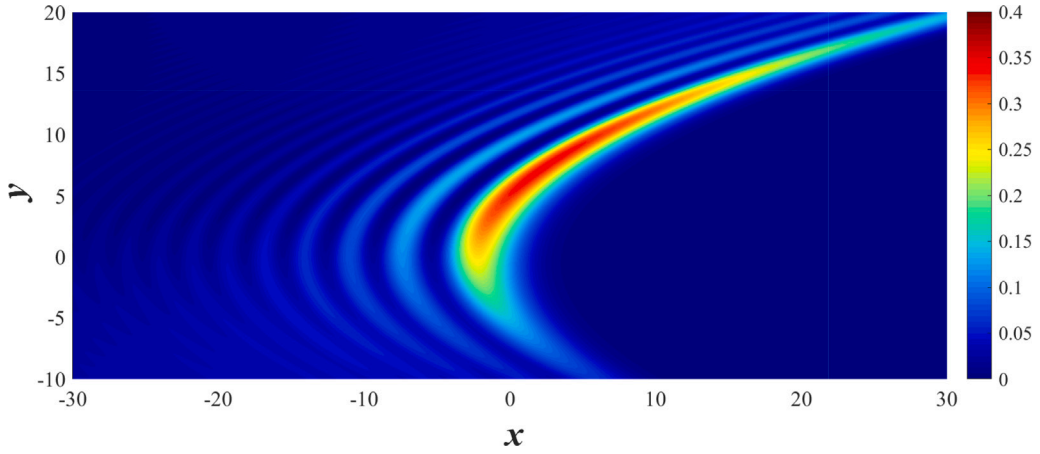

Fig. S3. Visualization of the squared modulus of the asymmetric function (A.10) $|\phi^+|^2$ with $a_1 = 1$ and $a_2 = 1/20$ at $t = 1$. This function decays exponentially in space but is asymmetric.

This function and its complex-conjugate provide the highly localized ripplon solution derived in this paper through the auxiliary function (5.2) (cf. Eq. (5.1) for ϕ^+). The spatial structure of the function $|\phi^+|^2$ is shown in Fig. S2 for $\rho = 1$, $a_1 = 1$, and $t = 1$.

With other choices of constants a_1 and a_2, one can obtain a variety of different solutions. One of them with asymmetric spatial structure of function $|\phi^+|^2$ is shown in Fig. S3 that was generated for $\rho = 1$, $\mathrm{Rt}\left(Z^3 + i/12t\right) = i/\sqrt[3]{12t}$, $a_1 = 1$ and $a_2 = 1/20$. The corresponding function ϕ^+ is:

$$\phi^+ = \frac{\rho}{\sqrt[3]{t}}\mathrm{Ai}\left[\frac{1}{\sqrt[3]{12t}}\left(x - 12ia_2 + \frac{a_1^2 + 4y(ia_1 - y)}{48}\right)\right] \times \exp\left[\frac{x\left(a_1 + iy\right) + 12a_2\left(2y - ia_1\right)}{24t} + \frac{a_1^3/6 + ia_1^2 y - 2a_1 y^2 - 4iy^3/3}{288t^2}\right]. \tag{A.11}$$

References

[1] M. Ablowitz, H. Segur, Solitons and the Inverse Scattering Transform, SIAM, Philadelphia, 1981.
[2] S. Novikov, M. S.V., L. Pitaevsky, Z. V.E., Theory of Solitons. The Inverse Scattering Method, Consultants Bureau, NY and London, 1984.
[3] V. Matveev, M. Salle, Darboux Transformations and Solitons, vol. 17, Springer, 1991.
[4] S. Manakov, V. Zakharov, L. Bordag, A. Its, V. Matveev, Two-dimensional solitons of the Kadomtsev–Petviashvili equation and their interaction, Phys. Lett. A 63 (3) (1977) 205–206.
[5] M. Ablowitz, J. Satsuma, Solitons and rational solutions of nonlinear evolution equations, J. Math. Phys. 19 (10) (1978) 2180–2186.
[6] A. Zaitsev, Formation of stationary nonlinear waves by superposition of solitons, Sov. Phys. Dokl. 28 (1983) 720–722.
[7] S. Gdanov, B. Trubnikov, Soliton chains in a plasma with magnetic viscosity, JETP Lett. 39 (1984) 129–132.

[8] D. Pelinovsky, Y. Stepanyants, New multisoliton solutions of the Kadomtsev–Petviashvili equation, JETP Lett. 57 (1993) 24–28.
[9] W. Hu, W. Huang, Z. Lu, Y. Stepanynats, Interaction of multi-lumps within the Kadomtsev–Petviashvili equation, Wave Motion 77 (2018) 243–256.
[10] A.C. Newell, L.G. Redekopp, Breakdown of Zakharov–Shabat theory and soliton creation, Phys. Rev. Lett. 38 (8) (1977) 377–380.
[11] J.W. Miles, Obliquely interacting solitary waves, J. Fluid Mech. 79 (1) (1977) 157–169.
[12] J.W. Miles, Resonantly interacting solitary waves, J. Fluid Mech. 79 (1) (1977) 171–179.
[13] K. Gorshkov, D. Pelinovsky, Y. Stepanyants, Normal and anomalous scattering, formation and decay of bound states of two-dimensional solitons described by the Kadomtsev–Petviashvili equation, JETP 77 (2) (1993) 237–245.
[14] C. Lester, A. Gelash, D. Zakharov, V. Zakharov, Lump chains in the KP-I equation, Stud. Appl. Math. 147 (4) (2021) 1425–1442.
[15] J. Rao, K.W. Chow, D. Mihalache, J. He, Completely resonant collision of lumps and line solitons in the Kadomtsev–Petviashvili I equation, Stud. Appl. Math. 147 (3) (2021) 1007–1035.
[16] J. Rao, J. He, B.A. Malomed, Resonant collisions between lumps and periodic solitons in the Kadomtsev–Petviashvili I equation, J. Math. Phys. 63 (1) (2022).
[17] Y.A. Stepanyants, D. Zakharov, V. Zakharov, Lump interactions with plane solitons, Radiophys. Quantum Electron. 64 (10) (2022) 665–680.
[18] R. Johnson, S. Thompson, A solution of the inverse scattering problem for the Kadomtsev-Petviashvili equation by the method of separation of variables, Phys. Lett. A 66 (4) (1978) 279–281.
[19] A. Nakamura, Decay mode solution of the two-dimensional KdV equation and the generalized Bäcklund transformation, J. Math. Phys. 22 (11) (1981) 2456–2462.
[20] A. Nakamura, Simple similarity-type multiple-decay-mode solution of the two-dimensional Korteweg-de Vries equation, Phys. Rev. Lett. 46 (12) (1981) 751.
[21] Z. Zhang, X. Yang, Q. Guo, Y. Cao, Rare decaying ripple solutions within the KP equation, Physica D (2023) 133920.
[22] V. Zakharov, A. Shabat, A scheme for integrating the nonlinear equations of mathematical physics by the method of the inverse scattering problem. I, Funct. Anal. Appl. 8 (3) (1974) 226–236.
[23] J. Satsuma, Soliton solution of the two-dimensional Korteweg–de Vries equation, J. Phys. Soc. Japan 40 (1976) 286–290.
[24] J. Satsuma, M. Ablowitz, Two-dimensional lumps in nonlinear dispersive systems, J. Math. Phys. 20 (3) (1979) 1496–1503.
[25] L. Abramyan, Y. Stepanyants, Two-dimensional multisolitons: Stationary solutions of Kadomtsev–Petviashvili equation, Radiophys. Quantum Electron. 28 (1) (1985) 20–26.
[26] N. Singh, Y. Stepanyants, Obliquely propagating skew KP lumps, Wave Motion 64 (2016) 92–102.
[27] L. Guo, A. Chabchoub, J. He, Higher-order rogue wave solutions to the Kadomtsev–Petviashvili 1 equation, Physica D 426 (2021) 132990.
[28] F. Calogero, A. Degasperis, Solution by the spectral-transform method of a nonlinear evolution equation including as a special case the cylindrical KdV equation, Lett. Nuovo Cimento 23 (1978) 150–154.
[29] F. Calogero, A. Degasperis, Spectral Transform and Solitons: Tools to Solve and Investigate Nonlinear Evolution Equations, North- Holland Pub. Co., Amsterdam, Holland, 1982.
[30] A. Nakamura, H.-H. Chen, Soliton solutions of the cylindrical KdV equation, J. Phys. Soc. Japan 50 (1981) 711–718.
[31] W. Hu, J. Ren, Y. Stepanyants, Solitary waves and their interactions in the cylindrical Korteweg–de Vries equation, Symmetry 15 (2) (2023) 413.
[32] W. Hu, Z. Zhang, Q. Guo, Y. Stepanyants, Solitons and lumps in the cylindrical Kadomtsev–Petviashvili equation. Part 1: Axisymmetric solitons and their stability, Chaos 34 (2024) 013138.
[33] R.S. Johnson, Water waves and Korteweg–de Vries equations, J. Fluid Mech. 97 (4) (1980) 701–719.
[34] V. Golin'ko, V. Dryuma, Y. Stepanyants, Nonlinear quasicylindrical waves: exact solutions of the cylindrical Kadomtsev–Petviashvili equation, in: Nonlinear and Turbulent Processes in Physics, Proc. 2-Nd Int. Workshop on Nonlin. and Turbul. Processes in Phys., Kiev, 1983, Harwood Academic Publishers, Gordon and Breach, 1984, pp. 1353–1360.
[35] Y. Stepanyants, On the connections between solutions of one-dimensional and quasi-one-dimensional evolution equations, Russian Math. Surveys 44 (1) (1989) 255–256.
[36] Z. Zhang, W. Hu, Q. Guo, Y. Stepanyants, Solitons and lumps in the cylindrical Kadomtsev–Petviashvili equation. Part 2: Lumps and their interactions, Chaos 34 (2024) 013132.
[37] V.D. Lipovskii, V.B. Matveev, A.O. Smirnov, Connection between the Kadomtsev–Petviashvili and Johnson equations, J. Sov. Math. 46 (1) (1989) 1609–1612.
[38] G.A. Siviloglou, D.N. Christodoulides, Accelerating finite energy Airy beams, Opt. Lett. 32 (8) (2007) 979–981.